2007 IEEE International Conference on
Robotics and Automation
Roma, Italy, 10-14 April 2007

Level-Ground Walk Based on Passive Dynamic Walking for a Biped Robot with Torso

Terumasa Narukawa, *Graduate Student Member, IEEE*, Masaki Takahashi, *Member, IEEE*, and Kazuo Yoshida

***Abstract*— This study presents a design technique of an efficient biped walking robot on level ground with a simple mechanism based on passive-dynamic walking. A torso is used to generate active power replacing gravity used in passive walk. Swing-leg control is introduced to create a steady gait. Numerical simulations show that a biped robot with knees and a torso can walk efficiently on level ground. When we choose an appropriate parameter of the swing-leg control, the biped robot can walk stably over a wide range of speed. Furthermore, the walking performance of the robot increases with the increase of the radius of circular feet.**

I. Introduction

Utilizing the dynamical property of a robot system is a useful approach to achieve an efficient walking. Passive-dynamic walking first studied by McGeer [14] is a solution. McGeer showed that a biped robot without actuators and controllers can walk stably down a shallow slope in numerical simulations and experiments. Passive walkers exhibit stable gaits, which are not planned in advance depending on the robot dynamics and a slope angle. The usefulness of passive-dynamic walking for an efficient walking robot leads many studies of biped robots on level ground based on passive walkers, e.g. [5].

Passive walkers can only walk on a shallow slope. On level ground, active walking should be studied. The mechanical energy is mainly lost through the swing-leg impacts with the ground at heel strike. The energy loss is recovered by using gravitational potential energy in the case of passive-dynamic walking. On level ground, active power source replacing gravity is necessary. McGeer has proposed various methods of energy input based on passive-dynamic walking as follows [13] [15]:

1) Applying torque at the ankle joint and the hip joint.
2) Applying an impulsive push when the stance-leg leaves the ground.
3) Varying leg length.
4) Utilizing reaction torque against a leaning torso.

Although ankle torque is mainly used for control e.g. [2] [3] [8] [16], and can imitate passive walking mechanism [1] [3], it has drawback from the viewpoints of zero moment point condition, discussed in [3]. Instead of the ankle torque, using a torso would be worth studying [13] [15].

This study aims at establishing a design technique of an efficient biped walking robot on level ground with a simple mechanism. We focus on passive walking mechanism to achieve efficient walking with a simple mechanism. We propose a level-ground walking by using a torso and swing-leg control based on passive walk. Although the use of the torso to recover the energy lost through the heel strike was proposed [13], there are few studies to use the torso explicitly for a biped robot on level ground based on passive walking. In addition to that, we introduce the swing-leg control in order to satisfy the condition of heel strike, which is essential to create a steady gait.

In this paper, numerical simulations show that a biped robot with a torso and knees on level ground can walk stably and efficiently at various speeds by using the torso and swing-leg control. In particular, the swing-leg control is important to walk over a wide range of speed. Furthermore the effects of circular feet are confirmed.

II. Level-Ground Walk Based on Passive Walking Mechanism

A. Passive-Dynamic Walking

Although the simplest passive walker is composed of only two mass-less links and one mass at hip [7], the simplest biped can walk stably. The gait is stable if all sufficiently small perturbations in the states of the gait converge without falling down. From the simplest walking, passive dynamic walking mechanisms are summarized as follows:

1) The stance-leg acts as an inverted pendulum and the robot moves forward.
2) The swing-leg acts as a free pendulum and hits the ground before the robot falls down. That is, swing-leg motion is to avoid falling down.
3) Energy supply should be required because the impact causes a loss of kinetic energy. In the case of passive walking, the energy loss is recovered by using potential energy to walk down a slope.

Passive walk mechanisms show that stable gaits can be

Manuscript received September 15, 2006. This work was supported in part by Grant-in-Aid for Exploratory Research, 17656082 from the Ministry of Education, Culture, Sports, Science and Technology. The work of the first author was supported by Grant-in-Aid for JSPS Fellows, 1853073 from Japan Society for the Promotion of Science.

Terumasa Narukawa is with Graduate School of Science and Technology, Keio University, Yokohama, 223-8522 Japan (corresponding author e-mail: narukawa@2003.jukuin.keio.ac.jp).

Masaki Takahashi and Kazuo Yoshida are with Department of System Design Engineering, Keio University, Yokohama, 223-8522 Japan (e-mail: takahashi@sd.keio.ac.jp; yoshida@sd.keio.ac.jp).

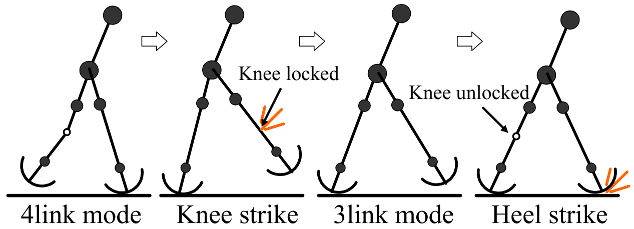

Fig. 1 The gait cycle of a biped robot with knees

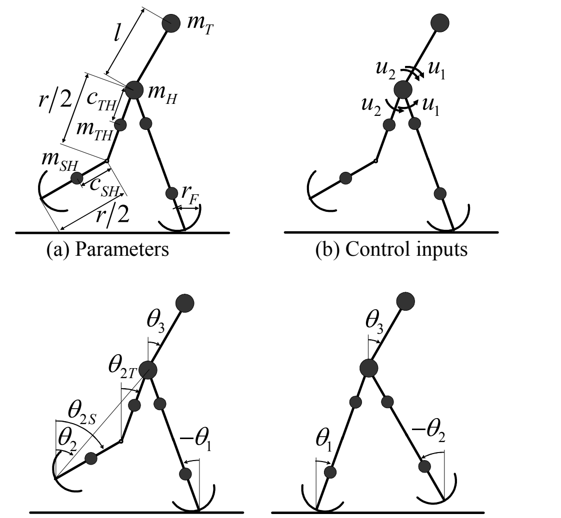

(a) Parameters (b) Control inputs

(c) Dynamic variables. 4link mode (left), 3link mode (right).

Fig. 2 A biped walking model. The robot is composed of a torso, hips, and two legs composed of thighs and shanks with feet. All masses are lumped. Dynamic variable values are measured from ground normal. Two torques u_1 and u_2, between the torso and the stance-leg, and between the torso and the swing-leg are applied, respectively. No torque is applied at the knee in the 4link mode. When the swing-leg reaches full extension the knee joint is locked and the knee remains locked through stance phase. Then we model the biped robot using the 4link mode before knee strike, corresponds to the 3link mode after knee strike. The motion of the robot is constrained to the sagittal plane.

realized simply by the stance-leg motion with energy supply and the swing-leg motion, but passive walkers have some limitations. The gaits depend on a slope angle. The walking speed decreases with the slope angle. Increasing the slope angle brings about a period doubling bifurcation leading to chaotic gaits and there are only unstable gaits in high speed region. Then, some mechanisms are required to overcome the limitations. This issue will be addressed in the proposed method.

B. Proposed Method for Level-Ground Walking

We propose a level-ground walking based on passive walking mechanisms mentioned in the previous section to overcome the limitations of passive walking.

First, we assume that when the knee of the swing-leg reaches full extension, so called knee-strike, the knee joint is locked and the knee remains locked through stance phase. Before knee strike we model the system using the 4 link mode, while after knee strike corresponds to the 3 link mode as shown in Fig. 1. The locking mechanism on a real robot has been realized, e.g. using a latch disengaged by a solenoid [4].

Second, we add a torso to the biped robot. To hold the torso which leans forward against the gravity, we apply a torque between the stance-leg and the torso. This leads to generating a forward-rotating torque at stance-leg. In this way, the kinetic energy which is mainly lost through the swing-leg impacts with the ground at heel strike is recovered. It should be noted that using the torso replacing gravity used in the case of passive-dynamic walking was proposed by McGeer [13]. By using the torso, a desired torso angle plays a similar role of the slope angle of passive walk. Then the robot can walk at various speeds by changing the desired torso angle.

Finally, we introduce a swing-leg control which modifies the natural pendulum motion of the swing-leg to walk stably over a wide range of speed. The swing-leg control is important to avoid falling down. The swing-leg control overcomes the limitation of passive walk which is only unstable gaits in high speed region, e.g. [7]. Wisse *et al.* showed that the robot will never fall forward if the swing-leg is far enough in front of the stance-leg but the swing-leg shouldn't be too far [18]. From this viewpoint, we propose that the swing-leg control should depend on the stance-leg motion because the impact condition of the swing-leg depends on the stance-leg. That is, the swing-leg control is applied in order to satisfy the impact condition.

TABLE I VALUES OF THE SYSTEM PARAMETERS

Parameter	Unit	Value	Parameter	Unit	Value
m_{TH}	kg	3	r	m	1
m_{SH}	kg	2	l	m	0.5
m_H	kg	10	c_{TH}	m	0.3
m_T	kg	10	c_{SH}	m	0.3
g	m/s^2	9.80665	r_F	m	0/0.1/0.2/0.3

III. BIPED ROBOT MODEL

The level-ground walking based on passive walk proposed in this paper needs a torso. A biped robot with a torso shown in Fig. 2, is considered. Values of the system parameters are shown in Table I.

A. Swing Phase

The dynamic model during swing phase is obtained by the method of Lagrange [10]. The swing model of the 4link mode is written in the form

$$ {}^4M\left({}^4\boldsymbol{\theta}\right){}^4\ddot{\boldsymbol{\theta}} + {}^4C\left({}^4\boldsymbol{\theta}, {}^4\dot{\boldsymbol{\theta}}\right){}^4\dot{\boldsymbol{\theta}} + {}^4G\left({}^4\boldsymbol{\theta}\right) = {}^4B\mathbf{u} \quad (1) $$

where ${}^4\boldsymbol{\theta} = \left[\theta_1 \;\; \theta_{2T} \;\; \theta_{2S} \;\; \theta_3\right]^T$, $\mathbf{u} = \left[u_1 \;\; u_2\right]^T$, and

$$ {}^4B = \begin{bmatrix} -1 & 0 \\ 0 & -1 \\ 0 & 0 \\ 1 & 1 \end{bmatrix}. \quad (2) $$

The model of the 3link mode is written in the form

$$ {}^3M\left({}^3\boldsymbol{\theta}\right){}^3\ddot{\boldsymbol{\theta}} + {}^3C\left({}^3\boldsymbol{\theta}, {}^3\dot{\boldsymbol{\theta}}\right){}^3\dot{\boldsymbol{\theta}} + {}^3G\left({}^3\boldsymbol{\theta}\right) = {}^3B\mathbf{u} \quad (3) $$

where ${}^3\boldsymbol{\theta} = \left[\theta_1 \ \theta_2 \ \theta_3\right]^T$, $\mathbf{u} = \left[u_1 \ u_2\right]^T$, and

$$ {}^3B = \begin{bmatrix} -1 & 0 \\ 0 & -1 \\ 1 & 1 \end{bmatrix}. \quad (4) $$

The details of the matrices M, C, and G in (1) and (3) are omitted due to space restriction.

B. Impact Phase

Impacts occur when the knee of the swing-leg reaches full extension and when the swing-leg touches the ground.

1) *Knee Strike:* The condition of the impact is given by

$$ \theta_{2T} = \theta_{2S}. \quad (5) $$

The impact is assumed to be inelastic. Angular momentum is conserved at the impact [6] [9] [14]for the whole robot about the stance-leg contact point, for the torso about the hip, and for the swing-leg about the hip. The conservation law of the angular momentum leads to the following compact equation between the pre- and post-impact angular velocities

$$ Q^{K+}\left({}^3\boldsymbol{\theta}^{K+}\right){}^3\dot{\boldsymbol{\theta}}^{K+} = Q^{K-}\left({}^4\boldsymbol{\theta}^{K-}\right){}^4\dot{\boldsymbol{\theta}}^{K-}. \quad (6) $$

The superscripts "$\mathrm{K}-$" and "$\mathrm{K}+$" respectively denote pre- and post-impact of the knee. During the impact phase of the knee, the configuration remains unchanged. Then we have

$$ {}^3\dot{\boldsymbol{\theta}}^{K+} = Q^{K+}\left({}^4\boldsymbol{\theta}^{K-}\right)^{-1} Q^{K-}\left({}^4\boldsymbol{\theta}^{K-}\right){}^4\dot{\boldsymbol{\theta}}^{K-}. \quad (7) $$

The details of the matrices are omitted due to space restriction.

2) *Heel Strike:* The condition of the impact is given by

$$ \theta_1 + \theta_2 = 0. \quad (8) $$

The impact is assumed to be inelastic and without slipping, and the stance-leg lifts from the ground without interaction [10] [11]. Angular momentum is conserved at the impact [6] [9] [14] for the whole robot about the new stance-leg contact point, for the torso about the hip, for the new swing-leg about the hip, and for the shank of the new swing-leg about the knee of the new swing-leg. The conservation law of the angular momentum leads to the following compact equation between the pre- and post-impact angular velocities:

$$ Q^{H+}\left({}^4\boldsymbol{\theta}^{H+}\right){}^4\dot{\boldsymbol{\theta}}^{H+} = Q^{H-}\left({}^3\boldsymbol{\theta}^{H-}\right){}^3\dot{\boldsymbol{\theta}}^{H-}. \quad (9) $$

The superscripts "$\mathrm{H}-$" and "$\mathrm{H}+$" respectively denote pre- and post-impact of the heel. During the impact phase, the configuration remains unchanged. Then the pre- and post-impact angles are identified with

$$ {}^4\boldsymbol{\theta}^{H+} = \begin{bmatrix} 0 & 1 & 0 \\ 1 & 0 & 0 \\ 1 & 0 & 0 \\ 0 & 0 & 1 \end{bmatrix} {}^3\boldsymbol{\theta}^{H-}. \quad (10) $$

From (9) and (10) we have

$$ {}^4\dot{\boldsymbol{\theta}}^{H+} = Q^{H+}\left({}^3\boldsymbol{\theta}^{H-}\right)^{-1} Q^{H-}\left({}^3\boldsymbol{\theta}^{H-}\right){}^3\dot{\boldsymbol{\theta}}^{H-}. \quad (11) $$

The details of the matrices are omitted due to space restriction.

IV. Torso and Swing-Leg Control

A. Torso Control

To hold the torso around a desired angle by applying the torque of the torso, τ_T, the simple PD control scheme given by

$$ \tau_T = -k_T^P\left(\theta_3 - \theta_3^d\right) - k_T^D\dot{\theta}_3 \quad (12) $$

is considered [13]. θ_3^d is the desired torso angle, k_T^P and k_T^D are control gain. k_T^P and k_T^D are determined as follows [13]. If the legs are firmly planted on the ground, the linearized equation of the torso motion with the PD control about $\theta_3 = 0$ becomes

$$ m_T l^2\ddot{\theta}_3 + k_T^D\dot{\theta}_3 + \left(k_T^P - m_T g l\right)\theta_3 = 0. \quad (13) $$

The frequency of the torso is

$$ \hat{\omega}_T = \sqrt{\frac{k_T^P - m_T g l}{m_T l^2}}. \quad (14) $$

The damping ratio is

$$ \hat{\zeta}_T = \frac{k_T^D}{2 m_T l^2 \hat{\omega}_T}. \quad (15) $$

On the other hand, if the stance-leg is firmly planted on the ground and the knee of the swing-leg is locked, the linearized equation of the swing-leg motion about $\theta_2 = 0$ becomes

$$ I_S\ddot{\theta}_2 + \left(m_{TH} g c_T + m_{SH} g\left(\tfrac{1}{2}r + c_S\right)\right)\theta_2 = 0 \quad (16) $$

where

$$ I_S = m_{TH} {c_T}^2 + m_{SH}\left(\tfrac{1}{2}r + c_S\right)^2. \quad (17) $$

The natural frequency of the swing-leg is

$$ \omega_S = \sqrt{\frac{m_{TH} g c_T + m_{SH} g\left(\frac{1}{2}r + c_S\right)}{I_S}}. \quad (18) $$

In this paper, the torso control parameters, k_T^P and k_T^D, are determined to satisfy

$$ \hat{\omega}_T = 3\omega_S, \quad (19) $$

$$ \hat{\zeta}_T = 0.7. \quad (20) $$

B. Swing-Leg Control

In order to satisfy the transition condition (8) before the robot falls down by applying the torque of the swing-leg, τ_S, we use the simple control law given by

$$ \tau_S = -k_S^P\left(\theta_2 - \left(-\theta_1\right)\right). \quad (21) $$

The swing-leg control leads to modifying the natural motion of the swing-leg. Note that, in the control law, $-\theta_1$ becomes the desired angle of the swing-leg, which is opposed to the spring model between the legs [12] [17]. If the stance-leg angle is constant and the knee of the swing-leg is locked, the linearized equation of the swing-leg motion with the swing-leg control about $\theta_2 = 0$ becomes

$$ I_S\ddot{\theta}_2 + \left(k_S^P + m_{TH} g c_T + m_{SH} g\left(\tfrac{1}{2}r + c_S\right)\right)\theta_2 = 0. \quad (22) $$

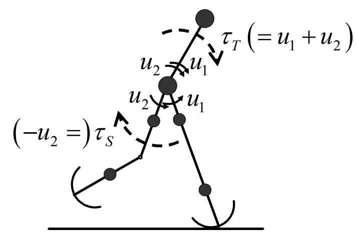

Fig. 3 Relationship between the desired torque, τ_T, τ_S, and the control inputs, u_1, u_2.

The frequency is

$$\hat{\omega}_S=\sqrt{\frac{k_S^P+m_{TH}gc_T+m_{SH}g\left(\frac{1}{2}r+c_S\right)}{I_S}}\,. \tag{23}$$

k_S^P is determined to satisfy

$$\hat{\omega}_S=K\omega_S\,. \tag{24}$$

K is a new swing-leg control parameter which shows the ratio between the frequencies of the swing-leg with the swing-leg control and without the swing-leg control. We will investigate the effect of the swing-leg control parameter, K later.

C. Control Inputs

From the torso and the swing-leg control, the control inputs are given by

$$u_1=\tau_T+\tau_S\,, \tag{25}$$

$$u_2=-\tau_S\,, \tag{26}$$

as shown in Fig. 3.

V. Simulation Results

By using the Newton-Raphson method, we can find stable or unstable period-one gaits [7]. In addition to that, we search period-doubling bifurcations of stable gaits to increase the desired torso angle from 0.01rad in steps of 0.001rad. The simulations were run by using MATLAB®/SIMULINK®. We use ODE45 and specify a scalar relative error tolerance of 1e-8 and an absolute error tolerance of 1e-8. The heel strike of the biped robot was detected by zero-crossing detection in SIMULINK®.

A. Definition of Gait Characteristics

The main gait characteristics of interest in this paper are speed and energetic cost. We define the characteristics of the gait as follows. Average walking speed is defined as

$${}^{k}v=\frac{{}^{k}x_{CM}^{+}-{}^{k-1}x_{CM}^{+}}{{}^{k}T} \tag{27}$$

where T is the step period, x_{CM} is the center of mass of the robot, the superscript "k" denotes step number, and "$+$" denotes post-impact between the swing-leg and the ground. An average input power is defined as [3]

$$p=\frac{1}{T}\int_0^T\left(\left|\left(\dot{\theta}_3-\dot{\theta}_1\right)u_1\right|+\left|\left(\dot{\theta}_3-\dot{\theta}_{2T}\right)u_2\right|\right)dt\,. \tag{28}$$

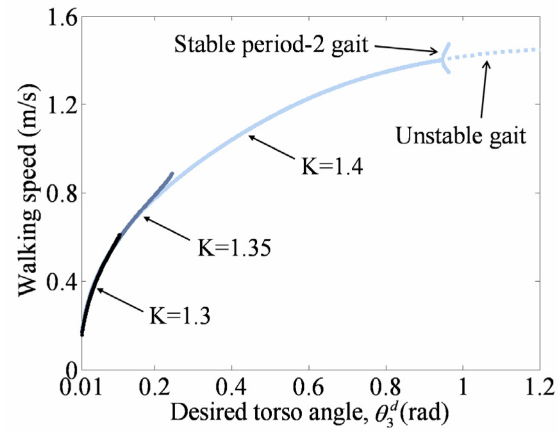

(a)

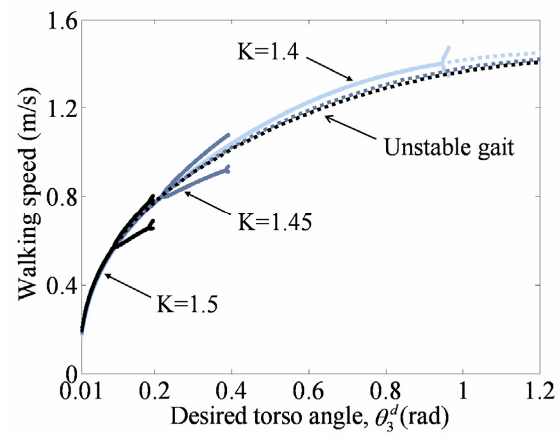

(b)

Fig. 4 Simulation results of the robot walking without circular feet i.e. $r_F=0$. Walking speed as a function of the desired torso angle where (a) K=1.3, 1.35, and 1.4, (b) K=1.4, 1.45, and 1.5.

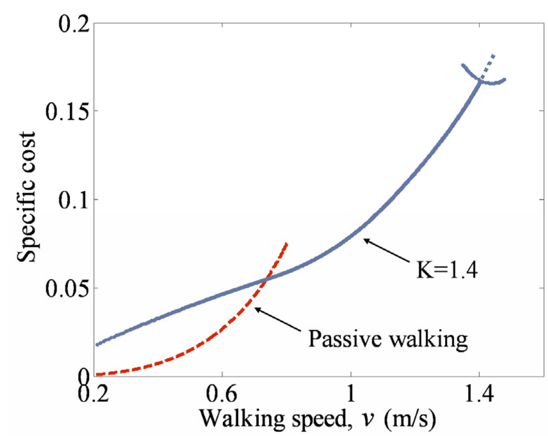

Fig. 5 Simulation results of the robot walking without circular feet i.e. $r_F=0$. Specific cost of transport as a function of the walking speed where K= 1.4 compared with passive walking.

Note $\dot{\theta}_{2T}$ is replaced with $\dot{\theta}_2$ in the case of the 3 link mode. The specific cost of transport is defined as

$$SpecificCost=\frac{p}{\left(2m_{TH}+2m_{SH}+m_H+m_T\right)gv}\,. \tag{29}$$

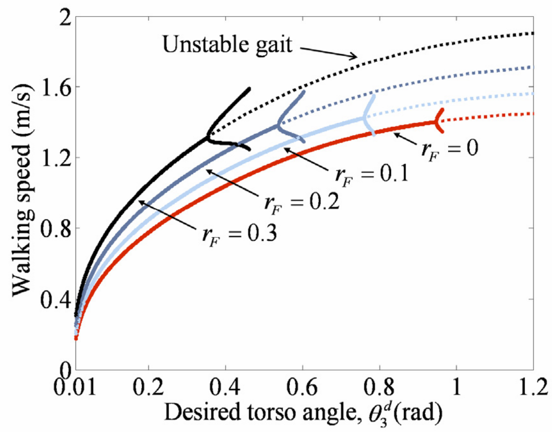

Fig. 6 Walking speed as a function of the desired torso angle where $r_F = 0$, 0.1, 0.2, and 0.3. In all cases, the swing-leg control parameter, *K*=1.4.

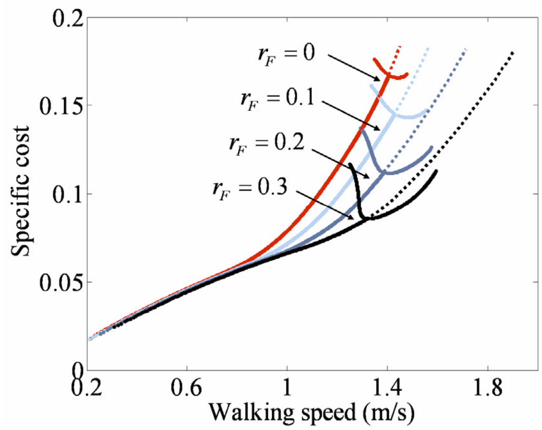

Fig. 7 Specific cost of transport as a function of the walking speed where $r_F = 0$, 0.1, 0.2, and 0.3 compared with passive walking. In all cases, the swing-leg control parameter, *K*=1.4.

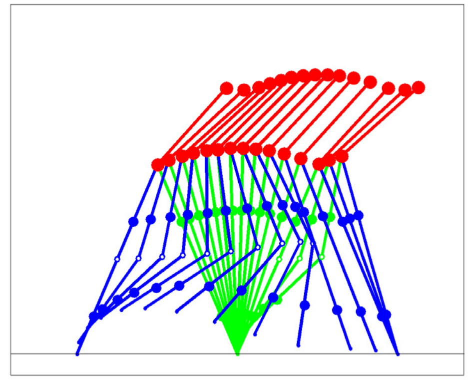

(a)

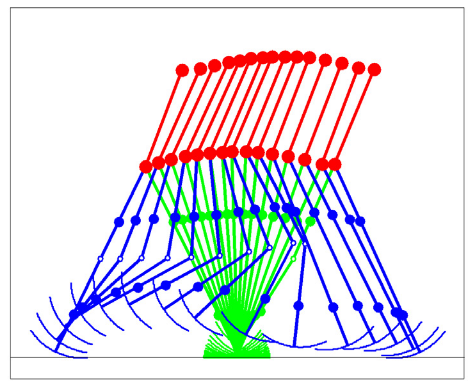

(b)

Fig. 8 Stick diagrams from just after a heel strike to after the next heel strike. (a) $r_F = 0$ and $\theta_3^d = 0.7$. The walking speed is about 1.3m/s. The specific cost of transport is 0.14. (b) $r_F = 0.3$ and $\theta_3^d = 0.35$. The walking speed is about 1.3m/s which is the same of case (a). The specific cost of transport is 0.09, i.e. more efficient walking than case (a).

B. Walking Performance of the Biped Robot without Circular Feet

First, we confirm the effectiveness of the swing-leg control in the case of the biped robot without circular feet, i.e. $r_F = 0$. We search a stable walking when only the torque between the stance-leg and the torso is applied, while the swing-leg is left free, i.e. $K = 1$. In the search, a steady gait is not found. Then we introduce the swing-leg control. Fig. 4 shows the evolution of the walking speed as a function of the desired torso angle where the swing-leg control parameters, $K = 1.3$, 1.35 , 1.4 , 1.45, and 1.5. Fig. 4(a) demonstrates that a stable waking is realized by introducing the swing-leg control and the maximum walking speed of the stable gait increases with the swing-leg control parameter. Note that when we increase further the swing-leg control parameter, K , period-doubling bifurcations occur and the maximum walking speed doesn't necessarily increase with the swing-leg control parameter as shown in Fig.4(b). From Fig. 4, the walking speed increases with the desired torso angle. Then the desired torso angle plays a similar role of the slope angle of passive walk. In Fig. 5, the efficiency of locomotion on level-ground is compared with passive walking of the compass-model [9]. The specific cost of transport of passive walking is just equal to $\sin\gamma$ where γ is the slope angle [14]. From Fig. 5, we conclude that the proposed method enables the biped robot on level ground to walk efficiently over a wide range of speed because the specific cost of transport is about as small as the passive-dynamic walking.

C. The Effects of the Circular Feet

In this section, we investigate the effects of the circular feet. Fig. 6 shows that the walking speed increases with the radius of the circular feet at an equal desired torso angle. Fig. 7 shows that when the walking speed is high the specific cost of transport decreases with the increase of the radius of the circular feet. Fig. 8 shows stick diagrams of biped walking with circular feet and without the feet. In each case, the walking speed is about 1.3 m/s. The desired torso angle of the biped robot with circular feet is smaller than without the feet. The specific cost of transport of the biped robot with circular feet is smaller than without the feet.

VI. Conclusion

By using the torso and swing-leg control, the biped walking robot on level ground exhibits stable and efficient gaits which are not planned in advance. In particular, by introducing the swing-leg control, the biped robot can walk stably over a wide range of speed. Furthermore the simulations show that the increase of the radius of the circular feet increases walking performance.

References

[1] F. Asano and M. Yamakita, "Virtual Gravity and Coupling Control for Robotic Gait Synthesis," *IEEE Trans. Systems, Man, and Cybernetics Part A*, vol. 31, no. 6, pp. 737-745, 2001

[2] F. Asano, M. Yamakita, N. Kamamichi, and Z.-W. Luo, "A novel gait generation for biped walking robots based on mechanical energy constraint," *IEEE Trans. Robotics and Automation*, vol. 20, no. 3, pp. 565-573, 2004.

[3] F. Asano, Z.-W. Luo, and M. Yamakita, "Biped gait generation and control based on a unified property of passive dynamic walking," *IEEE Trans. Robotics*, vol. 21, no. 4, pp. 754-762, 2005.

[4] S. H. Collins and A. Ruina, "A Bipedal Walking Robot with Efficient and Human-Like Gait," in *Proc. 2005 IEEE Int. Conf. Robotics and Automation*, Barcelona, Spain, April 2005, pp. 1983-1988.

[5] S. H. Collins, A Ruina, R. Tedrake, and M. Wisse, "Efficient bipedal robots based on passive-dynamic walkers," *Science*, 307, pp. 1082-1085, 2005.

[6] M. Garcia, "Stability, scaling and chaos in passive-dynamic gait models," Ph.D. dissertation, Cornell University, Ithaca, NY, 1999.

[7] M. Garcia, A. Chatterjee, A. Ruina, and M. Coleman, "The simplest walking model: stability, complexity, and scaling," *J. Biomechanical Engineering*, vol. 120, no. 2, pp. 281-288, 1998.

[8] A. Goswami, B. Espiau, and A. Keramane, "Limit cycles in a passive compass gait biped and passivity-mimicking control laws," *Autonomous Robots*, vol. 4, no. 3, pp. 273-286, 1997.

[9] A. Goswami, B. Thuilot, and B. Espiau, "Compass-like biped robot-part I: stability and bifurcation of passive gaits," Technical Report 2996, INRIA, 1996.

[10] J. W. Grizzle, G. Abba, and F. Plestan, "Asymptotically stable walking for biped robots: analysis via systems with impulse effects," *IEEE Trans. Automatic Control*, vol. 46, no. 1, pp. 51-64, 2001.

[11] Y. Hurmuzlu and D. B. Marghitu, "Rigid body collisions of planar kinematic chains with multiple contact points," *Int. J. Robotics Research*, vol. 13, no. 1, pp. 82-92, 1994.

[12] A. D. Kuo, "Energetics of actively powered locomotion using the simplest walking model," *J. Biomechanical Engineering*, vol. 124, pp. 113-120, 2002.

[13] T. McGeer, "Stability and control of two-dimensional biped walking," Technical Report CSS-IS TR 88-01, Simon Fraser University, 1988.

[14] T. McGeer, "Passive dynamic walking," *Int. J. Robotics Research*, vol. 9, no. 2, pp. 62-82, 1990.

[15] T. McGeer, "Dynamics and control of bipedal locomotion," *J. Theoretical Biology*, vol. 163, no. 3, pp. 277-314, 1993.

[16] M. W. Spong and F. Bullo, "Controlled symmetries and passive walking," *IEEE Trans. Automatic Control*, vol. 50, no. 7, pp. 1025-1031, 2005.

[17] M. Wisse, A. L. Schwab, and F. C. T. van der Helm, "Passive dynamic walking model with upper body," *Robotica*, vol. 22, pp. 681-688, 2004.

[18] M. Wisse, A. L. Schwab, R. Q. van der Linde, and F. C. T. van der Helm, "How to keep from falling forward: elementary swing leg action for passive dynamic walkers," *IEEE Trans. Robotics*, vol. 21, no. 3, pp. 393-401, 2005.